Current Applied Physics 12 (2012) 860–864

Contents lists available at SciVerse ScienceDirect

Current Applied Physics

journal homepage: www.elsevier.com/locate/cap

The effect of gamma irradiation on electrical and dielectric properties of Al-TiW-Pd_2Si/n-Si Schottky diode at room temperature

İlbilge Dökme [a,*], Şemsettin Altındal [b]

[a] Science Education Department, Faculty of Gazi Education, Gazi University, Ankara, Turkey
[b] Physics Department, Faculty of Arts and Sciences, Gazi University, 06500 Teknikokullar, Ankara, Turkey

ARTICLE INFO

Article history:
Received 26 July 2011
Accepted 23 November 2011
Available online 3 December 2011

Keywords:
Radiation effects
Al-TiW-Pd_2Si/n-Si
Dielectric properties
Ac electrical conductivity
Interface states

ABSTRACT

The effects of ^{60}Co (γ-ray) irradiation on the electrical and dielectric properties of Al-TiW-Pd_2Si/n-Si Schottky diodes (SDs) have been investigated by using capacitance–voltage (C–V) and conductance –voltage (G/ω–V) measurements at room temperature and 500 KHz. The corrected capacitance and conductance values were obtained by eliminating the effect of series resistance (R_s) on the measured capacitance (C_m) and conductance (G_m) values. The high–low frequency capacitance (CHF–CLF) method given in [12] as $N_{ss} = (1/qA)\,[((1/C_{LF}) - (1/C_{ox}))^{-1} - ((1/C_{HF}) - (1/C_{ox}))^{-1}]$ was successfully adapted to the before-after irradiation capacitance given in this report as $N_{ss} = (1/qA)\,[((1/C_{bef}) - (1/C_{ox}))^{-1} - ((1/C_{after}) - (1/C_{ox}))^{-1}]$ for the analyzing the density of interface states. The N_{ss}–V plots give a distinct peak corresponding to localized interface states regions at metal and semiconductor interface. The experimental values of the ac electrical conductivity (σ_{ac}), the real (M') and imaginary (M'') parts of the electrical modulus were found to be strong functions of radiation and applied bias voltage, especially in the depletion and accumulation regions. The changes in the dielectric properties in the depletion and accumulation regions stem especially from the restructuring and reordering of the charges at interface states and surface polarization whereas those in the accumulation region are caused by series resistance effect.

1. Introduction

It is well-known the metal-semiconductor (MS) or metal–insulator–semiconductor (MIS) type SDs, metal-oxidesemiconductor (MOS) capacitors, and solar cells are extremely sensitive to high level radiation such as ^{60}Co γ-ray, electrons or ions. Radiation generates electron-hole pairs in the interfacial insulator that subsequently interact with trapping sites within the interfacial layer. These radiation-generated electrons either recombine with the holes or move out of the interfacial layer. On the other hand, the radiation generated holes may diffuse in the interfacial layer, but are less mobile than the electrons; many stationary traps are also present. When there is an electric field present, the electrons will readily move out of the interfacial layer, and the trapping of holes becomes considerably enhanced [1]. Recently, it has been found by researchers that radiation response of MIS and MOS structures changes significantly when these structures are exposed to irradiation stress treatments [2–7]. They observed that the influence of high-level radiation such as γ-rays on these semiconductor devices produces lattice defects and hence quasi-stable changes happen in the electrical and dielectric properties of such devices.

The chip containing 14 dots of Al-TiW-Pd_2Si/n-Si Schottky diodes with the areas of changing 1×10^{-6} cm^2.to 14×10^{-6} cm^2 were fabricated by photolithographic technique and the electrical and dielectrical characteristics of Al-TiW-Pd_2Si/n-Si Schottky diodes were analyzed and reported in our previous studies [8–10]. This paper presents the effect of ^{60}Co γ-ray irradiation (22 kGy) on the electrical and dielectric properties of Al-TiW-Pd_2Si/n-Si Schottky diodes for the investigating of the radiation response of this device. We measured forward and reverse bias C–V and G/ω–V characteristics at room temperature and 500 kHz before and after irradiation in order to achieve a better understanding of the effects of ^{60}Co γ-ray irradiation (22 kGy) on the electrical and dielectric properties of Al-TiW-Pd_2Si/n-Si Schottky diodes. The voltage dependence of R_s and N_{ss} profiles, ac electrical conductivity (σ_{ac}) and real (M') and imaginary (M'') parts of the electric modulus of the diodes were investigated before and after irradiation.

* Corresponding author. Tel.: +90 312 2155471; fax: +90 386 2134513.
E-mail address: ilbilgedokme@gazi.edu.tr (İ. Dökme).

1567-1739/$ – see front matter © 2011 Elsevier B.V. All rights reserved.
doi:10.1016/j.cap.2011.11.021

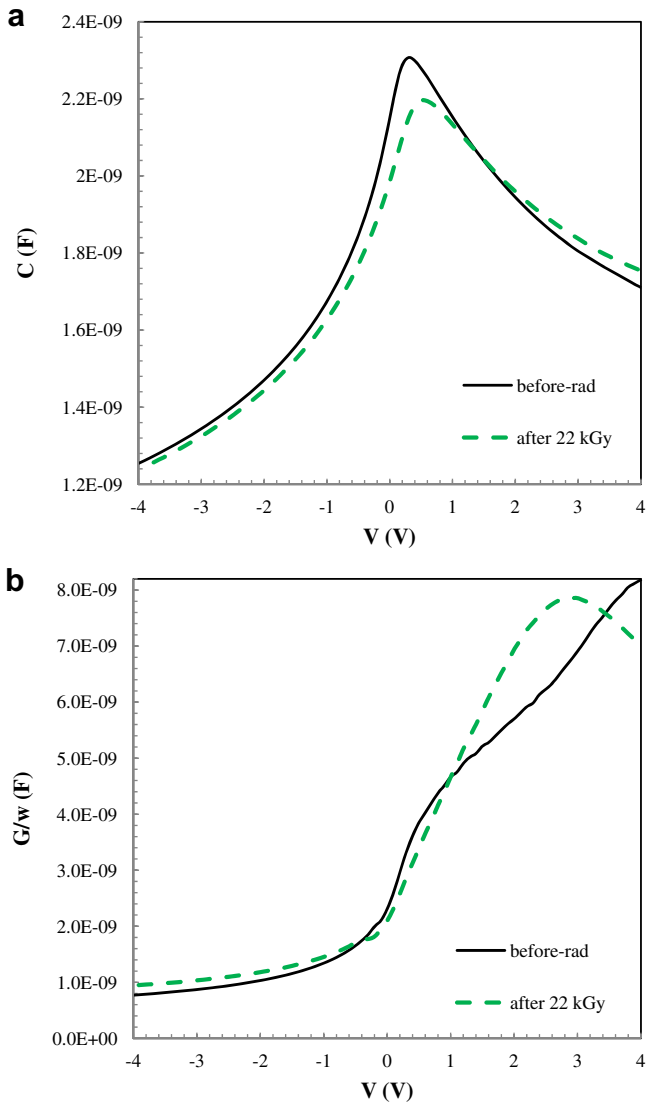

Fig. 1. The measured (a) C–V (b) G/ω–V characteristics of Au Al-TiW-Pd_2Si/n-Si SD before and after radiation.

2. Experimental procedure

The Al-TiW-Pd_2Si/n-Si diodes were fabricated on 2 inch diameter n-type (P doped) single crystal silicon wafer with (111) surface orientation, 0.7 Ω cm resistivity and 3.5 μm thickness. The pattern of these diodes were fabricated by photolithographic technique, defined as photo-resist, and annealed at 500 C for 1 min in flowing dry nitrogen (N_2) ambient in a rapid thermal annealing furnace. Thus produced chip contains 14 Al-TiW-Pd_2Si/n-Si diodes with the areas of changing 1×10^{-6} cm^2.to 14×10^{-6} cm^2. Only the results of diode with the area of 8×10^{-6} cm^2 are presented in this paper.

For the fabrication process the Si wafer first was cleaned in a mix of a peroxide–ammoniac solution in 10 min and subsequent quenched in de-ionized water of resistivity of 18 MΩ cm for a prolonged time. After the cleaning process, high purity (99.999%) Al with a thickness of about 2000 Å were thermally evaporated onto whole back side of Si wafer at a pressure about 10^{-6} Torr in high vacuum system. The ohmic contacts were formed by annealing them for a few minutes at 450 °C. To fabricate Pd_2Si layer, palladium was deposited on Si wafer by using thermal evaporation method at 250 °C. At this temperature the Pd deposited in the exposed contact regions reacts to form Pd_2Si. The unconverted Pd was etched away with an aqueous solution of KI + I_2, an etchant which does not attack Pd_2Si, and subsequently annealed at 573 K for 15 min. The thickness of Pd_2Si was determined to be about 0.6 μm by use of the spectroscopic ellipsometry system (Jobin Yvon-Horiba). To form the metal electrodes (rectifier and ohmic contacts), traditionally Al dot could have been formed on Pd_2Si-nSi structure. But Al has high diffusion ability and it can lead to degrade contact's quality. Therefore in this work, to prevent the disadvantage of Al diffusion to n-Si, the TiW alloy played the role of the diffusion barrier between Pd_2Si, and Al was deposited on Pd_2Si-nSi layer. For this process, the sandwiched structure Al-$Ti_{10}W_{90}$ was deposited by the magnetron sputtering method at temperature of 420 °C in vacuum system 'Oratoria-5' and then annealed at temperature of 500 °C in nitrogen atmosphere (N_2) for 20 min.

Prior to the deposition, vacuum and target conditions were performed. Taking into account the dispersion factor of Ti and W, the compound target (Ti 10%, W 90%) was made. The deposition chamber was pumped down to the ultimate vacuum and repeatedly charged with argon and pumped down in order to minimize the residual gas components. The alloy compound target film was bombarded by Ar^+ ions with high energy at room temperature until the thickness of $Ti_{10}W_{90}$ film on Pd_2Si-nSi substrate was about 0.2 μm. The base pressure during the ion bombardments was about 10^{-6} Torr. Al was also deposited onto TiW-Pd_2Si/n-Si diodes by the same method until the thickness of Al film on $Ti_{10}W_{90}$-Pd2Si-nSi layer was about 1 μm.

The C–V and G/ω–V measurements of Al-TiW-Pd_2Si/n-Si diodes were performed at 500 kHz before and under ^{60}Co γ-ray source by using a HP 4192A LF impedance analyzer (5 Hz–13 MHz) and small sinusoidal test signal of 40 $mV_{p-p.}$ from the external pulse generator. All measurements were carried out with the help of a microcomputer through an IEEE-488 ac/dc converter card.

3. Results and discussion

The plots of the measured C–V and G/ω–V of the Al-TiW-Pd_2Si/n-Si SDs before and after irradiation at room temperature and 500 kHz and they are given in Fig. 1 (a) and (b), respectively. As shown in Fig. 1 (a) and (b), both C–V and G/ω–V characteristics exhibit inversion, depletion and accumulation regions. The range of

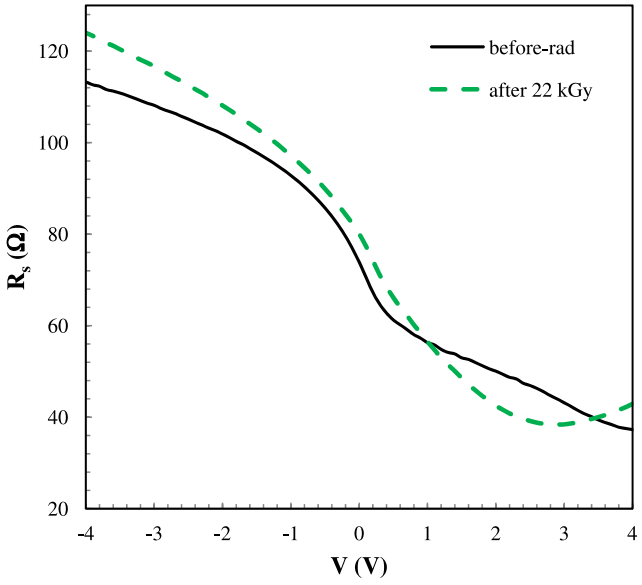

Fig. 2. The R_s characteristics of Al-TiW-Pd_2Si/n-Si SD before and after radiation.

the applied bias voltage is −4 V to 4 V. It can be seen in Fig. 1(a) that the values of C increase under the effect of γ radiation in accumulation region whereas they decrease in the depletion and the inversion regions. Also, there is a peak in both plots (before and after irradiation) of C–V at about 0.3 V because of the effect of R_s. Such behavior shows that the N_{ss} is the significant parameter in the depletion and weak accumulation regions whereas the significant parameter in the strong accumulation region is R_s. As can be seen in Fig. 1 (a) and (b), there is a discrepancy in the values of C and G/w due to radiation induced interface states. In order to eliminate the effect of R_s on C and G/w, R_s–V plots were obtained from the C–V and G/w–V measurements at 500 kHz using the following equation [11] and are given in Fig. 2.

$$R_s = \frac{G_{ma}}{G_{ma}^2 + (\omega C_{ma})^2} \tag{1}$$

where C_m and G_m are the values of measured capacitance and conductance at a given bias voltage, respectively. These significant values require that special attention should be given to the effects of R_s in the applications of the admittance-based C–V and G/w–V measurement methods. It is clear seen in Fig. 2 that the values of R_s considerable increase in the inversion and depletion regions with the effect of radiation while they decrease in the depletion region. We considered that the trap charges have enough energy to escape from the traps located between metal and semiconductor interface in the Si band gap. Also, at high frequencies, $f \geq 500$ kHz, the charges at the interface states cannot follow an ac signal [4,6].

The obtained series resistance values are used to correct the measured C–V and G/ω–V values. Therefore, measured capacitance and conductance values were corrected by eliminating the effect of R_s in order to obtain the real capacitance C_c and conductance G_c/ω values of the diode under reverse and forward bias. The corrected capacitance C_c and conductance G_c values are calculated using the following relations [11]

$$C_c = \frac{\left[G_m^2 + (wC_m)^2\right]C_m}{a^2 + (wC_m)^2} \tag{2}$$

and

$$G_c = \frac{\left[G_m^2 + (wC_m)^2\right]a}{a^2 + (wC_m)^2} \tag{3}$$

where $a = C_m - [G_m^2 + (wC_m)^2]R_s$. After the correction is made, C–V and G/w–V plots with their corrected versions before and after irradiation are given in Fig. 3 (a) and (b), respectively. As can be seen in Fig. 3 (a), when the correction was made on the C–V plot, the values of C_c increase considerably especially in the depletion and accumulation regions. Moreover, after the correction C_c–V plots give two peaks; one of which is in the depletion region proving that the charge transfer can take place through the interface. The first peak is located at the low forward bias region and the second peak is located at the high forward bias region. Each of peaks shifts to the low forward bias region under the radiation effect. On the other hand, it is clear seen in Fig. 3 (b) that when the correction was made on the G_c/w–V plots, the values of G_c/w decrease considerably in the depletion and accumulation regions while they increase in inversion region.

The changes in C–V and G/w–V plots can be attributed to restructuring and reordering of interface charges located at metal and semiconductor interface under radiation effect. Both values of C and G/w increase in the accumulation region under radiation effect. This increase in C and G/w values is also attributed to the increase in ε' and ε'' values.

There are several methods which have been suggested to determine the N_{ss} profile of MIS type SDs [11–14]. Among them the advantageous one is the high–low frequency capacitance (C_{HF}–C_{LF}) method [12], since it permits determination of many properties of the interfacial layer, the semiconductor substrate and interface easily. With this method, N_{ss} can be extracted from its capacitance contribution to the measured experimental C–V curve. The equivalent capacitance is the series connection of C_{ox} and surface charge capacitance C_{sc}. In this study, we used C_{HF}–C_{LF} method with a slight change in the formula such that we used $C_{bef.}$ and C_{after} instead of C_{LF} and C_{HF}, respectively, in order to make the formula suitable for calculating N_{ss} values under the effect of irradiation. N_{ss} values are obtained using the following equation [12],

$$N_{ss} = \frac{1}{qA}\left[\left(\frac{1}{C_{bef}} - \frac{1}{C_{ox}}\right)^{-1} - \left(\frac{1}{C_{after}} - \frac{1}{C_{ox}}\right)^{-1}\right] \tag{4}$$

where $C_{bef.}$ And C_{after} are the values of capacitance before and after irradiation. The density distribution of N_{ss} profile as function of bias voltage was calculated from Eq. (4) and is given in Fig. 4. As shown

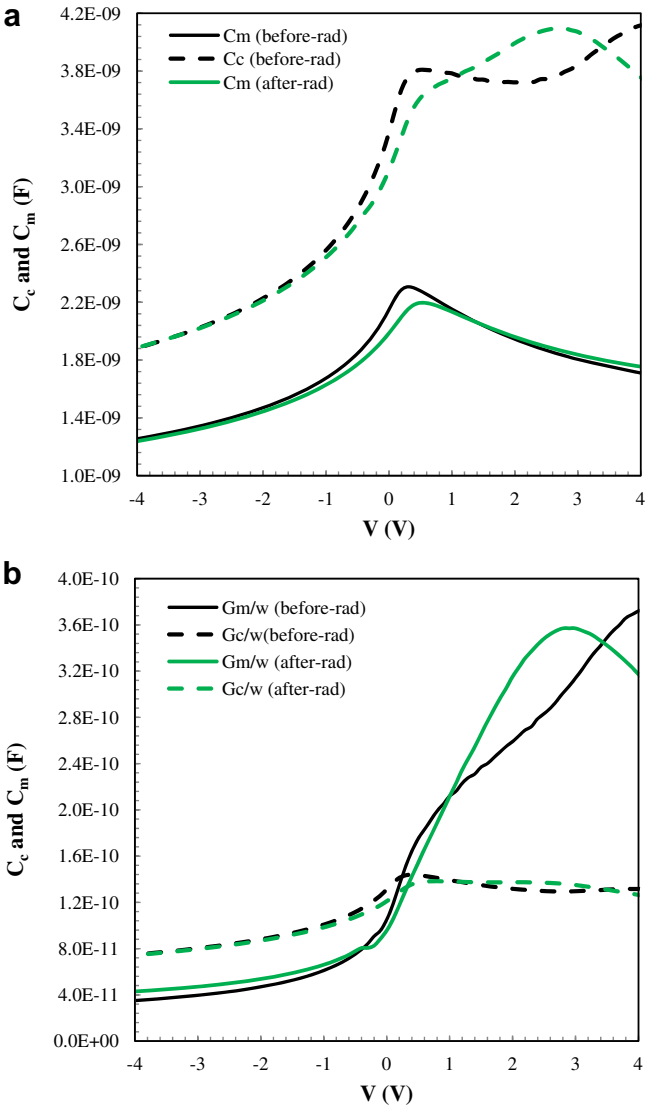

Fig. 3. The plots of the voltage dependent (a) C_c–V and (b) G_c/ω–V of Al-TiW-Pd_2Si/n-Si SD before and after radiation.

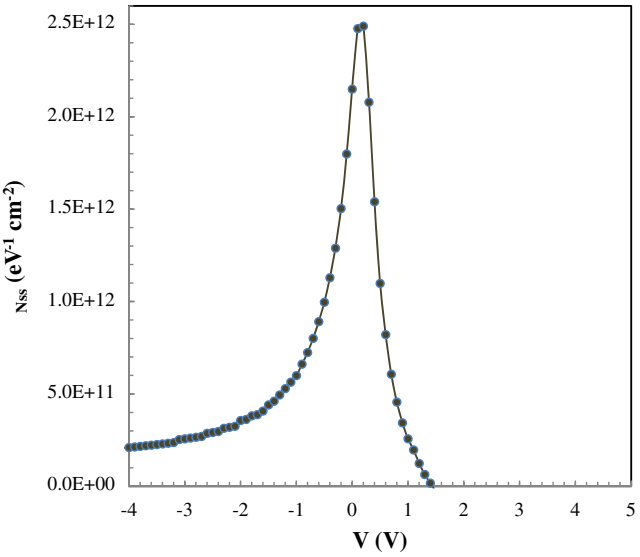

Fig. 4. The N_{ss} profile of -TiW-Pd_2Si/n-Si SD before and after radiation.

in Fig. 4, the plots of N_{ss} give a peak at about 0.1 V due to the radiation induced interface states and the peak value is about 2.48×10^{12} eV^{-1} cm^{-2}. Devices with this order of interface states are more suitable for the fabrication of electronic devices. Moreover, this result shows that the interface of Al-TiW-Pd_2Si/n-Si SD are more resistant to the radiation.

The basic dielectric parameters such as dielectric constant (ε'), dielectric loss (ε''), loss tangent ($\tan\delta$), ac electrical conductivity (σ_{ac}), the real (M') and imaginary (M'') parts of electric modulus can be express as following equations [15,16],

$$\varepsilon^* = \varepsilon' - i\varepsilon'' \tag{5}$$

$$\varepsilon^* = \frac{Y^*}{jwC_o} = \frac{C}{C_o} - i\frac{G}{wC_{o_i}} \tag{6}$$

$$\varepsilon' = \frac{C}{C_o} = \frac{Cd_i}{\varepsilon_o A} \tag{7}$$

$$\varepsilon'' = \frac{G}{wC_o} = \frac{Gd_i}{\varepsilon_o wA} \tag{8}$$

$$\tan\delta = \frac{\varepsilon''}{\varepsilon'} \tag{9}$$

$$\sigma_{ac} = wC\tan\delta(d/A) = \varepsilon'' w\varepsilon_o \tag{10}$$

where ε' and ε'' are the real and imaginary of complex permittivity (ε^*), and i is the imaginary root of $\sqrt{-1}$, Y^* is complex admittance, C and G are the measured capacitance and conductance of the device, w is the angular frequency ($w = 2\pi f$) of the applied electric field, $C_o = \varepsilon_o A/d_i$ is capacitance of an empty capacitor, A is the rectifier contact area of the structure in cm^{-2}, d_i is the interfacial insulator layer thickness and ε_o is the electric permittivity of free space ($\varepsilon_o = 8.85 \times 10^{-14}$ F/cm).

The complex impedance (Z^*) and complex electric modulus (M^*) formalisms were discussed by various authors with regard to the analysis of dielectric materials [17,18]. Analysis of the complex permittivity (ε^*) data in the Z^* formalism ($Z^* = 1/Y^* = 1/i\omega C_o\varepsilon^*$) is commonly used to separate the bulk and the surface phenomena and to determine the bulk dc conductivity of the material [17–19].

Many authors prefer to describe the dielectric properties of these devices by using the electric modulus formalize [17,18]. The complex impedance or the complex permittivity ($\varepsilon^* = 1/M^*$) data are transformed into the M^* formalism using the following relation [11,19]

$$M^* = i\omega C_o Z^* \tag{11}$$

or

$$M^* = \frac{1}{\varepsilon^*} = M' + jM'' = \frac{\varepsilon'}{\varepsilon'^2 + \varepsilon''^2} + j\frac{\varepsilon''}{\varepsilon'^2 + \varepsilon''^2} \tag{12}$$

The real component M' and the imaginary component M'' are calculated from ε' and ε''. The voltage dependent real (M') and imaginary part (M'') of electric modulus plots of Al-TiW-Pd_2Si/n-Si SD before and after irradiation are given in Fig. 5 (a) and (b), respectively. As can be seen these figures M' and M'' decrease

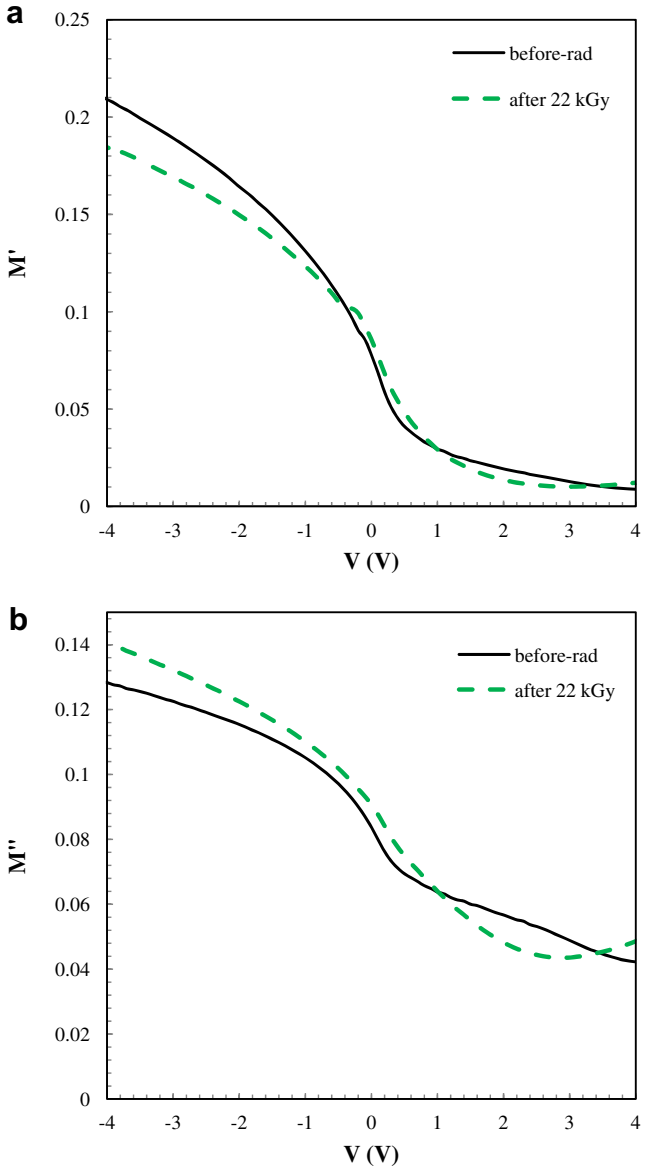

Fig. 5. The voltage dependence of (a) the real part (M') and (b) the imaginary part (M'') of electric modulus (M^*) at room temperature and 500 kHz for Al-TiW-Pd_2Si/n-Si SD before and after radiation.

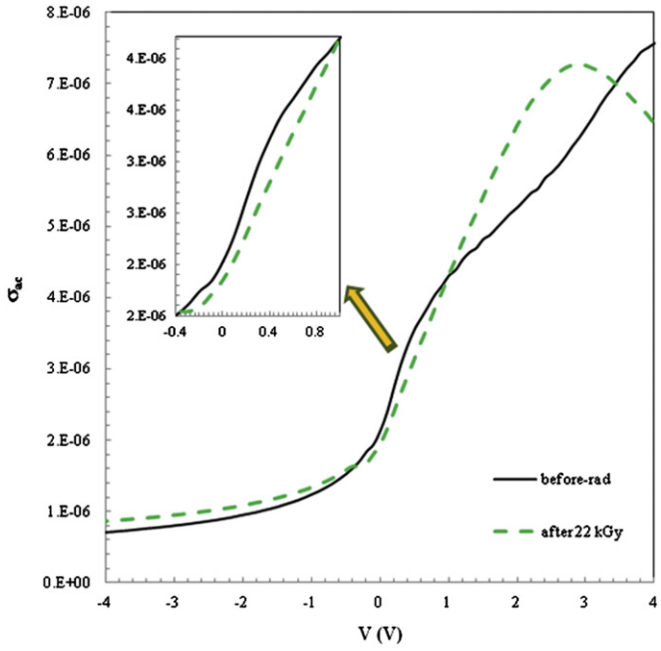

Fig. 6. The variation of the ac electrical conductivity σ_{ac} with applied bias for Al-TiW-Pd_2Si/n-Si SD before and after radiation.

considerably with increasing bias voltages. The values of M' decrease in the inversion region while they increase in the accumulation region under the effect of radiation. However, the values of M'' decrease in the inversion region while they increase in the accumulation region under the effect of radiation. It is interpreted that at 500 kHz the period (T) is very much lower than the lifetime (τ) of interface states. Therefore, the interface states cannot follow an ac signal and the electrical modulus reaches a maximum value corresponding to $M\infty = 1/\varepsilon'\infty$ because of the relaxation process [4,7]. M' and M'' plots with maximum value in low bias voltage and then decrease to a minimum value. The change in M' and M'' plots with the γ-ray irradiation and bias voltage indicate the N_{ss} is passivated [4].

In order to see the effect of γ-ray irradiation on ac conductivity, before and after irradiation of the σ_{ac}–V plots of the Al-TiW-Pd_2Si/n-Si SD were obtained by using Eq. (10) and are given in Fig. 6. It is seen clearly in Fig. 6 that σ_{ac} is dependent on the radiation and applied bias voltage for the measurement SD. As can be seen in Fig. 6 and the inset in Fig. 6, the values of σ_{ac} decrease in the depletion region while they increase in the strong accumulation and inversion regions under the effect of radiation. Moreover, after irradiation σ_{ac}–V plots have a peak at about 2.7 V which is similar the G/w–V plots in Fig. 1 (b). Such behavior of ac conductivity results from the changes in the conductance under radiation effect and these changes in the strong accumulation region are more distinctive compared to other regions [7].

4. Conclusions

In order to show the effects of γ-ray irradiation on the electrical and dielectric properties of Al-TiW-Pd_2Si/n-Si SD, the C–V and G/ω–V measurements were carried out at room temperature and 500 kHz and in the bias voltage range of −4 V to 4 V. Experimental results show that radiation is effective on the C and G values in the depletion, accumulation and inversion regions. The values of R_s decrease under radiation effect particularly in the accumulation region (between 1.5 and 3.5 V) because of the increase in the conductivity of the device. The voltage dependent N_{ss} profile was also obtained from the measured capacitance ($C_{bef.}$ and C_{after}) values method and the values of N_{ss} were found to be about in the order of 10^{12} eV^{-1} cm^{-2}. In addition, the real and imaginary parts of electrical modulus and ac electrical conductivity values were obtained from the measured C and G values before and after irradiation. The changes in the electrical and dielectric properties in the depletion and accumulation regions stem especially from the restructuring and reordering of the charges at interface states, series resistance of device and interfacial polarization. As a conclusion, electrical and dielectric properties of Al-TiW-Pd_2Si/n-Si SD are considerably dependent on the radiation and applied bias voltage.

References

[1] K.H. Zainninger, A.G. Holmes-Siedle, A survey of radiation effect in MIS devices, RCA Rev. (1967).
[2] R.K. Chauhan, P. Chakrabarti, Microelectron. J. 33 (2002) 197.
[3] M.Y. Feteha, M. Soliman, N.G. Gomaa, M. Ashry, Renew. Energy 26 (2002) 113.
[4] Ş Karataş, A. Türüt, Ş Altındal, Rad. Phys. Chem. 78 (2009) 130.
[5] R.M. Radwan, Nucl. Instr. Meth. Phys. Res. B 262 (2007) 249.
[6] İ. Dökme, P. Durmuş, Ş Altındal, Nucl. Instr. Meth. in Phys. Res. B 266 (2008) 791–796.
[7] A. Tataroğlu, Ş Altındal, Nucl. Instr. Meth. Phys. Res. B 254 (2007) 113–117.
[8] İM. Afandiyeva, İ Dökme, Ş Altındal, L.K. Abdullayeva, Sh.G. Askerov, Microelectron. Eng. 85 (2008) 365.
[9] I.M. Afandiyeva, İ Dökme, Ş Altındal, M.M. Bülbül, A. Tataroğlu, Microelectron. Eng. 85 (2008) 247.
[10] İ Dökme, Ş Altındal, I.M. Afandiyeva, Semicond. Sci. Technol. 23 (2008) 035003.
[11] E.H. Nicollian, J.R. Brews, Bell Syst. Tech. J. 46 (1976) 1055–1138.
[12] R. Castange, A. Vapaille, Surf. Sci. 28 (1) (1971) 157.
[13] M. Çakar, Y. Onganer, A. Türüt, Synth. Metals 126 (2002) 213.
[14] W.A. Hill, C.C. Coleman, Solid-State Electron. 23 (9) (1980) 987.
[15] V.V. Daniel, Dielectric Relaxation, Academic Press, London, 1967.
[16] C.P. Symth, Dielectric Behavior and Structure, McGraw-Hill, New York, 1955.
[17] P. Pissis, A. Kyritsis, Solid State Ion. 97 (1997) 105.
[18] K. Prabakar, S.K. Narayandass, D. Mangalaraj, Phys. Stat. Sol. A 199 (2003) 507.
[19] M.D. Migahed, M. Ishra, T. Famy, A. Barakat, J. Phys. Chem. Solid 65 (2004) 1121.